Platelet Rich Fibrin Augmented Versus Non-Augmented Glycerolized Bovine Pericardium and Polypropylene Mesh for Repairing of Large Abdominal Wall Defects

El-Husseiny, H. M.
Department of Surgery, Anesthesiology and Radiology
El-Maghraby, H. M.
Department of Surgery, Anesthesiology and Radiology
Alakraa, A. M.
Department of Surgery, Anesthesiology and Radiology
Kandiel, M. M. M.
Department of Theriogenology, Faculty of Veterinary,
Medicine, Benha University, Egypt

Abstract

This study aimed to evaluate the use of glycerolized bovine pericardium (GBP) compared to polypropylene mesh (PPM) in repairing of large abdominal wall defects in animal model, and to investigate the role of platelet rich fibrin (PRF) in promoting this repair. Fresh bovine pericardium collected from local abattoir were processed and preserved in 99.5% glycerol. PRF matrix was harvested from fresh autologous blood (10 ml) after centrifugation. Fullthickness, mid-ventral abdominal wall defects (6 × 10 cm) were surgically created in 36 healthy goats (9 goats/group) and were repaired with an equal size of GBP, PPM, GBP-PRF, or PPM-PRF. Qualitative and gray scale quantitative ultrasonography were adopted at day 1, 1, 2, 3, 4, 8 and 12 weeks post-implantation. Three goats per group were slaughtered at 4, 8 and 12 weeks post-implantation for further gross, histopathological and tensiometric (tensile strength, load at failure and strain %) evaluations. Ultrasonography revealed significant (P< 0.05) improvement of implant gray scale, low subcutaneous edema and reduction of skin implant distance in PRFaugmented groups. Besides, a substantial improvement of connective tissue covering, implant incorporation, new blood vessels formation, and reduction of the inflammatory cells infiltrations were observed. Tensiometric parameters were improved in GBP-PRF group compared to the other groups. In conclusion, the obtained results not only proved the superiority of GBP over PPM, but also the advantage of PRF-augmented over non-augmented implants in treatment of large abdominal wall defects. Ultrasonographic analysis provided a satisfactory tool to evaluate the healing process of the abdominal wall defects.

Keywords: Platelet Rich Fibrin, Glycerolized Bovine Pericardium, Polypropylene mesh, Hernioplasty, Hernia

Introduction

Surgical repair of large abdominal wall defects still becomes a significant problem and a challenge for the surgeon with recurrence being a common outcome (1, 2). Prosthetic hernia repair is very important to overcome this problem (3).

Polypropylene mesh (PPM) has been shown to be very suitable for the repair of large abdominal wall defects in human and different animals, as it is strong and with an excellent tissue incorporation (4). One of the most important drawbacks of polypropylene mesh is that it is associated with high rate of adhesion formation to the abdominal wall and underlying viscera (4). This may lead to further complications as intestinal obstruction, abdominal pain, and visceral fistulation (3, 5). Increased postoperative complications associated with the use of PPM has increased the attention toward the search for safe, cheap and available biodegradable prosthetic material of adequate tensile strength for repairing of large abdominal wall defects (6).

As a biomaterial, pericardium has been mostly used for cardio-vascular applications, such as: arterial and vascular grafts (7) and artificial heart valves implantation (8). It was used also, for the treatment of acquired cardiac pathologies, including post-infarction septal defects and reconstruction of mitral valve annulus or outflow obstruction (9). Recently, pericardium also used for the construction of novel bio-prostheses in non-cardiac treatments such as patches for vaginal or abdominal wall defects repairing, dural defects repairing or tracheoplasty (10).

Platelet Rich Fibrin (PRF) is a single fibrin membrane of immune and platelet concentrates that collects all blood components necessary for healing, immunity and minimizing postoperative inflammatory process (11,12). PRF matrix plays a direct role in angiogenesis as it contains 6 main angiogenesis soluble factors such as fibroblast growth factor basic (FGFb), vascular endothelial growth factor (VEGF), angiopoïetin and platelet-derived growth factor (PDGF) (13).

Ultrasonographic examination is an effective tool for the diagnosis of large abdominal wall defects, identification of the implants and postoperative monitoring of the subcutaneous inflammatory fluid until its complete resolution (14 , 15). Quantification of the ultrasonogram by histogram analysis can enhance interpretation of good quality images through using a high-speed digital analysis system and specialized software (16). They added that the ultrasonogram had 256 shades in the gray scale of the image used for quantitative assessment of the taken ultrasonograms from 0 (black / anechoic) to 255 (white / hyperechoic).

The objectives of this study are to evaluate the use of glycerolized bovine pericardium (GBP) compared to polypropylene mesh (PPM) in repairing of large abdominal wall defects in animal model, and to investigate the role of platelet rich fibrin (PRF) in enhancing this function. Moreover, to describe the application of ultrasonography in the diagnosis of large size abdominal wall defects, post-operative monitoring and

quantitative gray scale histogram assessment of implanted GBP with and without PRF compared to PPM with and without PRF.

Material and methods:

Thirty-Six clinically normal and apparently healthy goats were included in this study. their ages ranged between one to three years and their weights ranged between 20 -30 Kgs. These animals were purchased from different localities at Kalvobiva Governorate; Kept under the same circumstances, dewormed with Ivermectin 10 mg (Noromectin 1%, Norbrook Laboratories Limited, Northern subcutaneously at a dose rate of 0.2 mg/kg b. w. and Albendazole 2.5% (Albendazole 2.5%, Pharma Swede Co. for pharm. Ind., Cairo. Egypt) or ally at a dose rate of 10 mg/kg b. w. They were housed in a comfortable soft bedded stall and received water ad libitum and balanced ration of concentrate and hay. All the procedures were accomplished according to the ethics for humane treatment of animal use in research guidelines and complied with the relevant legislation of Faculty of Veterinary Medicine, Benha University, Egypt. The animals were divided into four groups (Nine goats per group).

Group 1: included animals implanted with Glycerolized Bovine Pericardium (GBP group). **Group 2**: included animals implanted with Polypropylene mesh **(HEINE MESH, 30cm x 30cm, HEINE MEDIZIN GmbH., Dusseldorf, Germany)** (PPM group). **Group 3** included animals implanted with Glycerolized Bovine Pericardium with Platelet Rich Fibrin (GBP-PRF group). **Group 4**: included animals implanted with Polypropylene mesh with Platelet Rich Fibrin (PPM-PRF group).

1. Pre-operative preparation

The food was withheld for 24 hours prior to surgery and the surgical site was prepared aseptically as usual. Animals were sedated using 2% Xylazine HCl (*Xylaject, Adwia Co., Cairo, Egypt*) in a dose rate of (0.01 mg/Kg B. wt.) and the operation seat was infiltrated using 2% lidocaine HCl (*Debocaine, Aldebiky Co., Cairo, Egypt*). The animals were controlled in dorsal recumbency.

2. Preparation of Glycerolized Bovine Pericardium (GBP)

Bovine Pericardial patches were processed and preserved according to the method described after (17).

3. Preparation of Platelet Rich Fibrin Matrix (PRF)

PRF Matrix was prepared according to the method described by **(18)**. Specimens from PRF were obtained and fixed in 10 % buffered formal solution, stained with (H&E) stain, and examined histologically in order to detect the platelets and fibrin network.

4. Operative Technique

Full thickness, mid-ventral abdominal wall defect was created in all goats at the level of the umbilicus through 12 cm length paramedian skin incision made about 2-3 cm

away from the mid line of the ventral abdominal wall. Skin was bluntly dissected away from the underlying subcutaneous tissues. The dissection was extended to expose the linea alba that was resected to create an artificial (6 x 10 cm) full thickness abdominal wall defect including the peritoneum. Hemostasis was achieved properly to control any bleeding. The prosthetic materials with suitable size proportional to the size of the defects were implanted using the intraperitoneal (Underlay) technique after (19). Omentalization (Omentopexy) was created through grasping a part of omentum that was sutured to the peripheries of the implant. The implant was sutured in position using chromic cat gut size 0 by simple interrupted suture pattern. PRF was added on the surface of the implant in PPM-PRF and GBP-PRF groups prior to skin closure. Skin incision was closed using braided silk size 1 and interrupted mattress suture pattern.

5. Post-Operative Care

Animals received an I/M course of antibiotic therapy with penicillin-streptomycin *(Norbrook Laboratories Limited, Northern Ireland)* at dose rate of 30.000 IU/Kg penicillin and 10 mg/Kg streptomycin for 5 days post operatively. Skin wound was daily dressed, and skin stitches were removed 14 days post operatively.

6. Post-Operative follow up and evaluation

The animals were kept under observation to detect any changes or complications and they were evaluated depending on ultrasonographic examination at day 1, 1, 2, 3, 4, 8 and 12 weeks post-implantation: Three goats from each group were slaughtered at 4, 8 and 12 weeks post operatively for further evaluations depending on gross pathological and histopathological examinations. Tensiometric evaluations were adopted at 8 and 12 weeks post operatively.

6.1. Ultrasonographic Evaluation

Ultrasonographic Examination was performed using a portable ultrasound machine (*Eickemyer, Magic 1500, Co., Ltd, UK*) with adjusted 5 MHz linear array transducer. The machine was set at 4.6 cm depth and 52 gain. prior to ultrasonographic examination. The animals were ultrasonographically examined according to (14). Quantitative assessment of implant gray scale (IGS), subcutaneous gray scale (SGS) and skin implant distance (SID) were achieved by image brightness analysis [on gray scale units from 0 (black) to 255 (white)] by using dedicated software Image J (NACL Co. Ltd., Tokyo, Japan) to obtain the mean gray value of the analyzed ultrasonographic image.

6.2. Tensiometric Evaluation

Transverse strips (4 cm width and 10 cm length) harvested from the implanted grafts after slaughtering at 8 and 12 weeks post operatively. These strips included the implanted prosthetic materials and bilateral adjacent body wall. Specimens were collected in containers of normal saline, transported to the laboratory in icebox, and the biomechanical testing was done within 3 hours of samples collection. They were

mounted into the grips for computer controlled mechanical testing using tensile strength testing apparatus (*Servo Universal Testing Machine, WAW-600, Beijing Sinofound Co., Ltd, China*). The clamps of tensometer were coated from inside by a piece of felt and tightened to avoid slipping of tissue specimens, then proximal and distal parts of specimens were secured on the two metal clamps of the tensometer. All specimens were loaded and elongated till failure at speed of 50 mm/min. Tensile strength (TS), Load at failure (LF) and Strain percent were recorded according to (2).

6.3. Macroscopic Examination

Gross evaluation of the implantation site was conducted after slaughtering of the animals at 4, 8 and 12 weeks post operatively post operatively. A rectangular 6 cm in width skin area was removed and the parietal surface of the implant was examined to detect the connective tissue covering. The implant was excised and reflected to examine the visceral surface to record the neovascularization, connective tissue covering and degree of adhesion. The numerical scores of adhesions ranged from 0 to 4 were evaluated according to Modified Hopkins adhesion score (**Table 1**) performed by (**20**).

6.4. Microscopic Examination

Specimens were collected from patch grafts after slaughtering of the animals in different groups at 4, 8 and 12 weeks following implantation, fixed in 10% formal saline for 24 hours for preparation of paraffin sections. Thin sections of 4 microns thickness were cut and stained with Hematoxylin and Eosin stain (H & E) for examination through the light electric microscope (21).

6.5. Statistical Analysis

The obtained results were tabulated and expressed as Mean ± Standard Error of Means (SEM). All statistical analyses were conducted by using IBM-SPSS (Ver. 23). For comparison of the data of different groups at the same time points after surgery, the obtained data were compared using One Way Analysis of Variance (ANOVA) and posthoc with Duncan multiple comparison test. For comparison of the data of the same group with the pre-surgical values, data were analyzed using One Way ANOVA and post-hoc with Dunnett multiple comparison procedure. In order to compare the data of two time points (8 weeks versus 12 weeks), independent student t-test was conducted.

Results

I. Ultrasonographic Examination

I.1. Qualitative ultrasonographic assessment

On B-scan, the implanted materials in different groups appeared as thin white hyperechoic lines surrounded by anechoic area representing the acute inflammatory fluid at first day post implantation.

In PRF augmented groups, PRF appeared as a small hypoechogenic area surrounding the implants.

There was gradual increase in the echogenicity of the prosthetic implants during the 1^{st} , 2^{nd} and 3^{rd} weeks post implantation. This was highly marked in PRF groups that also showed incomplete infilling of the implants with multiple hypoechogenic dots representing the newly formed connective tissue at 3^{rd} week post implantation. In PPM group, the echogenicity of the prosthetic implants revealed incomplete infilling of the implants with few hypoechogenic dots.

Subcutaneous fluid appeared as anechoic area surrounding the prosthetic implants in different groups at 1st week post implantation. It was markedly increase in GBP group, while in PPM group it was lower and in PPM-PRF and GBP-PRF group it was the lowest. At 2nd week post implantation, it showed increase in GBP group, while in PPM group it showed gradual resolution with presence of few hypoechogenic dots, but in PPM-PRF and GBP-PRF groups it showed complete resolution with presence of multiple hypoechogenic dots representing the newly formed connective tissue. At 3rd week post implantation, subcutaneous fluid showed gradual resolution in GBP group. Subcutaneous fluid showed complete resolution in GBP and PPM groups at 4th week post implantation.

At 8th and 12th weeks, ultrasonographic image of subcutaneous area revealed gradual increase in the echogenicity in different groups that revealed presence of multiple hypoechogenic to few hyperechogenic dots in subcutaneous area in non-PRF groups, while in PRF groups it revealed presence of multiple hyperechogenic dots in the subcutaneous area surrounding the implants (Fig. 1).

I.2.Quantitative ultrasonographic assessment

I.2.a. Implant Gray Scale (IGS)

The mean IGS within each group showed significant (p < 0.001) difference at different time points of the study. The recorded IGS means of all groups were tabulated in Table 3. Comparing between different groups verified that the mean IGS of non-PRF groups was significant (p < 0.001) higher than PRF groups at the $1^{\rm st}$ day post implantation, while that of PRF groups was significant (p < 0.001) higher than that of non-PRF groups at $1^{\rm st}$ and $2^{\rm nd}$ weeks post implantation. At $4^{\rm th}$ and $8^{\rm th}$ weeks post implantation, the mean IGS of GBP-PRF group was significantly (p < 0.01) higher than that of the other groups and still significant (p < 0.001) higher than other groups at $12^{\rm th}$ week post implantation. Moreover, the mean IGS of PPM-PRF group was significant (p < 0.01) higher than that of the other groups at $2^{\rm nd}$ week post implantation. (Table 2 & Fig. 1).

I.2.b. Subcutaneous Gray Scale (SGS)

The mean SGS within each group showed significant (p < 0.001) difference at different time points of the study. The recorded subcutaneous gray scale means (SGS) of all

groups were tabulated in Table 4. Comparing between different groups showed that the mean SGS of GBP and GBP-PRF groups was significant (p < 0.001) lower than PPM and PPM-PRF groups at the $1^{\rm st}$ day post implantation, but it was significantly (p < 0.01) higher in PRF groups than in non-PRF groups at $1^{\rm st}$ week post implantation. The mean SGS of PPM-PRF group was significant (p < 0.001) higher than the other groups at $2^{\rm nd}$, $3^{\rm rd}$, $4^{\rm th}$ and $8^{\rm th}$ weeks post implantation. At $12^{\rm th}$ week after implantation, the mean SGS of GBP group was significantly (p < 0.001) lower than that of the other groups (Table 3 & Fig. 1).

I.2.c. Skin Implant Distance (SID) [mm]

The recorded skin implant distance (SID) means of all groups were tabulated in Table 5. The mean SID of GBP and GBP-PRF groups was significant (p < 0.05) higher than that of PPM and PPM-PRF groups at the 1^{st} day post implantation. The mean SID of GBP group was significant (p < 0.005) higher than that of the other groups at 1^{st} , 2^{nd} , 3^{rd} and 4^{th} weeks post implantation. Moreover, it was still significantly (p < 0.05) higher than the other groups at 12^{th} week post implantation (Table 4).

II. Tensiometric Evaluation

The site of breakage (failure) of the tested specimens was either at the interface between implant and muscle or on the muscle itself at one end of the implant.

Tensiometric characters showed changes over time points of the experiment. Comparison between different groups showed that the mean of both tensile strength and load at failure of GBP-PRF and PPM-PRF groups was very highly significant (p < 0.001) at 8 weeks and extreme highly significant (p < 0.0001) at 12 weeks higher than that of GBP and PPM groups post implantation. **(Tables 5 &6 and Fig. 2)**.

The mean strain % showed no significant change between different groups at 8 weeks post implantation. The mean strain % of GBP and GBP-PRF groups tend to be significant (p = 0.065) higher than that of PPM-PRF group at the 12 weeks post implantation (Table 7 & Fig. 2).

III. Macroscopic Examination

At 4^{th} week post operatively, the parietal surface of different implanted materials was covered by a thin layer of fibrous connective tissue with good incorporation of the implants with the recipient abdominal wall. In GBP-PRF and PPM-PRF groups, outer thin neovascularization was observed. The connective tissue covering, and neovascularization increased gradually at 8^{th} and 12^{th} weeks post operatively and became more prominent in GBP-PRF and PPM-PRF than GBP and PPM groups. The borders of the implanted material at PPM group showed folding and irregularities that were absent in the other groups (Fig. 3).

Macroscopic examination of the visceral surface of the implanted materials at 4^{th} week post operatively revealed that they were encapsulated with fibrous connective tissue

which increased gradually at 8th and 12th months post operatively and became more prominent in GBP-PRF and PPM-PRF than GBP and PPM groups **(Fig. 4)**.

The degree of adhesion was more severe in PPM group than the others, but it was the mildest in GBP-PRF group. The adhesion score 0 (no adhesion) was recorded only in GBP-PRF and PPM-PRF groups. Score 3 was recorded in GBP and PPM groups, while score 4 was recorded only in PPM group where severe matted adhesion between the PPM and the intestines was observed and causing unavoidable serosal damage on dissection. Scores (3) and (4) were absent only in PRF augmented groups (Table 8 & Fig. 5).

IV. Microscopic Examination

Histological examination of native unprocessed bovine pericardium revealed its intact normal structure composed of a single layer of simple squamous epithelium and connective tissue mainly elastin and collagen. Collagen fibers were more abundant, with marked organization at different levels range from fibrils to laminates and fibers. The collagen appeared red with clear flattened fibroblasts containing peripheral nuclei. Microscopic picture of glycerolized bovine pericardium (GBP) revealed absence of the epithelial layer and presence only of few necrotic nuclei with the collagen fibers that appeared red in color. PRF appeared histologically as dense, mature, homogenous and well-organized light pink fibrin network with presence of blood platelets aggregates that were discoidal, red and non-nucleated cells (Fig. 6).

At 4th week after implantation, histological examination of GBP group showed normal intact histological structure of GBP formed of dense collagen fibers surrounded by few numbers of inflammatory cells infiltration. In PPM group, the inflammatory cells were widely scattered around mesh fibers. In PRF-augmented groups, there were focal areas of few numbers of inflammatory cells. The granulation tissue formation was observed in the form of newly formed loose fibrous tissue and few scattered round fibroblasts surrounded by thin collagen fibers. These fibers were more abundant in GBP group, immature in PPM group and more pronounced parallel collagen fibers with presence of fibroblastic cells appeared round to ovoid in shape in PRF-augmented groups.

At 8th week, the inflammatory cells were severely reduced and observed as focal areas of few inflammatory cells in Non PRF-augmented groups. They were completely reduced in PRF-augmented groups. The loose connective tissue was gradually changed to dense fibrous connective tissue with presence of round to ovoid fibroblasts in non PRF-augmented groups. Wide areas of dense and parallel oriented collagen proliferations were observed with presence of multiple ovoid fibroblasts surrounding the collagen fibers in PRF-augmented groups. The neovascularization started to appear within the fibrous tissue in PRF-augmented groups.

At 12th week, there was small focal areas of very few inflammatory cells aggregations in GBP group and they were mainly around mesh fibers in PPM group. The

inflammatory cells were completely absent in PRF-augmented groups. Granulation tissue formation was observed by presence of dense fibrous connective tissue formed mainly of collagen fibers with presence of spindle shape fibroblasts in non PRF-augmented groups. In PRF-augmented groups, there were fibroblastic cells and collagen proliferations. Collagen became denser, abundant and surrounding the multiple spindle shape fibroblasts that observed more elongated, with flattened nuclei. Neovascularization were observed within the fibrous tissue of non-PRF groups. Presence of multiple newly formed blood capillaries and vessels with their characteristic endothelial lining within the fibrous tissue in PRF-augmented groups (Fig. 7).

Discussion

Processing and preservation of bovine pericardium using glycerol was an efficient method for pericardial treatment and decellularization. Glycerolized bovine pericardium (GBP) was superior to lyophilized (freeze-dried) bovine pericardium in treatment of large abdominal wall defects (22). Results of the present study revealed that GBP was compatible and acceptable by the recipient tissue for long periods after implantation. This was attributed to successive decellularization of bovine pericardial tissue that leaves only the collagenous structure of extra-cellular matrix (ECM) that is common (non -antigenic) in different domestic animals (23). In our study, GBP implants showed less intense post implantation inflammatory reaction compared to PPM, this comes in line with that mentioned by (2,22).

Size of abdominal wall defect (6 x 10) cm created in goats when compared to the animal size is considered large and representative of large abdominal defects encountered in different large animals that require bridging of these large defects using prosthetic implants. This finding comes in line with (24).

In the present study, ultrasonographic examination of GBP and PPM groups at 1st week following implantation revealed presence of anechoic image representing inflammatory fluid surrounding the hyperechoic implants that was more obvious in GBP group than PPM group. Complete resolution of this fluid noticed at 2nd week post implantation in all groups. These findings were attributed to inadequate hemostasis or rough excessive dissection during defect repair (25). Sonogram of PRF-augmented groups at 1st week following implantation revealed presence of slight anechoic fluid surrounding the hyperechoic implant. This finding confirmed the anti-inflammatory effect of PRF (26). At 2nd, 3rd and 4th weeks following implantation, sonography of GBP and PPM groups showed gradual and slight improvement of echogenicity that was more obvious in GBP group. At 8th and 12th weeks, results revealed gradual filling of the defects by echogenic dots representing collagen fibers which was incomplete infilling of PPM pores with collagen fibers. These findings agree with (25). Ultrasonographic examination of PRF-augmented groups at 2nd, 3rd and 4th weeks following implantation revealed presence gradual but quick improvement of the echogenicity that was more obvious at 8th and 12th weeks following implantation and showed complete filling of the defects with hyperechoic dots. This occurred because PRF matrix enhances the healing and covering of the injured tissues as they affect the metabolism of epithelial cells and fibroblasts and enable them to extend toward and cover the wound faster (13).

Quantitative ultrasonographic assessment of implants in different groups showed that implant and subcutaneous gray scale were significant (p < 0.05) higher in PRF-augmented groups at different time points of the study. Seven different growth factors and cytokines are released from degranulation of PRF and have a necessary role in stimulation of the healing of soft and hard tissues (12). The quantitative assessment also showed that skin implant distance was significant (p < 0.05) lower in PRF-augmented groups at different time points of the study. PRF composed of platelet concentrates that collect all blood components have the ability to regulate the inflammatory process (11,12).

Tensiometric evaluation of different groups revealed that the site of breakage (failure) of all tested implant strips was between the implant and surrounding rectus muscles (implant -muscle interface). The tensile strength of the rectus muscles and the newly formed fascia is lower than that at the implant site (2). There was no significant (p < 0.05) change in the mean tensile strength and load at failure in GBP and PPM groups at 8th and 12th weeks post implantation. Both GBP and PPM were strong enough to keep the integrity of abdominal wall (2, 17 & 22). The mean tensile strength and load at failure of PRF-augmented groups were significant (p < 0.05) higher than those of GBP and PPM at 8th and 12th weeks post implantation. This finding comes in line with (27). The mean tensile strength and load at failure of all tested groups showed significant (p < 0.05) increase at the 12^{th} week higher than that at the 8th week post implantation. The abdominal wall becomes stronger during the late periods after implantation due to formation of new tissue around the implant (2). The mean strain (%) showed no significant (p < 0.05) change between different tested groups at 8th week following implantation. This coincides with (28) who recorded that there was no significant difference in strain between different graft types over time that reached 52 weeks.

Macroscopic picture of different implants showed that connective tissue covering and neovascularization were more prominent and gradually increased by time in GBP group than PPM group and this finding agrees with (2). Adhesion scores were higher and more intense in PPM group than GBP group as repairing of abdominal wall defects using PPM usually results in severe degrees of adhesions with the visceral organs that results in more complications as intestinal fistula (29) moreover, GBP could be used for repairing of abdominal wall defects without stimulating adhesions with underlying viscera as the adhesion only recorded between the peritoneal surface of GBP and the omentum and this was attributed this to ischemia or foreign bodies that may encountered during the implantation (17). Adhesion scores were lower in PRF-augmented groups and score 0 was recorded only in them. Using of PRP can result in

reduction of adhesion occurrence and degree (30) and this is due to the antiinflammatory characters of platelet rich concentrates (26).

Microscopic examination of unprocessed bovine pericardium revealed that it is composed of a single layer of lining epithelial cells (simple squamous epithelium) and connective tissue mainly elastin and collagen. The antigenicity of unprocessed boyine pericardium as a xenograft was attributed to its cellular structure (32). Histology of GBP revealed its a cellular structure with absence of the epithelial layer and presence only of few necrotic nuclei with the collagen biomatrix (ECM). This finding agrees with (23) who mentioned that, histological examination is very important to assess the efficacy of pericardial decellularization. Histopathological examination of PRF showed presence of dense, mature, homogenous and well-organized fibrin network with aggregates of blood platelets that appeared discoidal, red non-nucleated cells in color (31). Microscopic examination of GBP and PPM groups showed that inflammatory cells infiltration was lower in GBP group than PPM group and revealed its gradual decrease of it by time. These findings come in agreement with (2). Inflammatory cells infiltration was lower in PRF-augmented groups at 4th, 8th and 12th weeks following implantation. This finding coincides with (26) who attributed this result to the anti-inflammatory properties of platelet rich concentrates. Newly formed connective tissue was more abundant in GBP group than PPM group which was gradually increased by time. This comes in agreement with (2). It was more prominent, obvious, regular and abundant in PRF-augmented groups at 4th, 8th and 12th weeks following implantation. Platelet cytokines and growth promoters have the ability to propagate and improve the healing process, enhance cell proliferation and differentiation because of their capacity to stimulate cell migration and proliferation (specially by PDGFs) and induce fibrin matrix remodeling as well as secretion of a cicatricial collagen matrix (specially by TGF- β) (27). Neovascularization was more obvious in PRF-augmented groups at 8th week following implantation and increased in number and size at 12th week following implantation. PRF matrix plays a direct role in angiogenesis as it contains 6 main angiogenesis soluble factors such as fibroblast growth factor basic (FGFb), vascular endothelial growth factor (VEGF), angiopoïetin and platelet-derived growth factor (PDGF) (13).

Conclusion

The results proved the priority of Glycerolized Bovine Pericardium (GBP) and Platelet Rich Fibrin (PRF) augmented implants in treatment of large abdominal wall defects. PRF provided favorable results in enhancement of the healing process through enhancing neovascularization, increasing tissue deposition and incorporation., reducing postoperative inflammatory reaction and minimizing the post-operative complications such as adhesions and recurrences.

Ultrasonographic examinations using histogram gray scale analysis provided a satisfactory tool to post operatively evaluate the healing process of abdominal wall defects repaired using different prosthetic implants.

Conflict of interest

The authors have no conflict of interest to declare.

References

- [1] Abouelnasr, K. S., Zaghloul, A. E. and Karrouf, G. I. (2014): Comparative evaluation of glycerolized bovine pericardium implant with prolene mesh for closure of large abdominal wall defects in dogs. IJVR, 15 (3): 211-217.
- [2] AL-Asadi, R. N. and Hummadi, S. K. (2011): Ultrasonographic Evaluation of Hernioplasty of Experimentally Induced Large Ventro-lateral Hernia in Bucks. The Iraqi J. Vet. Med. 35 (2): 105- 112.
- [3] Badylak, S. F. (2007): The extracellular matrix as a biologic scaffold material. Biomaterials. 28: 3587-3593.
- [4] Banchroft, J. D.; Stevens, A. L. and Turner, D. R. (1996): Theory and practice of histological technique. 4th Ed., London, New York, Churchill Livingstone, San Francisco, Tokyo. Pp. 210-250.
- [5] Baptista, M. L.; Bonsack, M. S. and Delaney, J. P. (2000). Seprafilm reduces adhesions to polypropylene mesh. Surgery. 128: 86-92.
- [6] Bellon, J. M., Conteras, L. A., Pascual, G., and Bunjan, J. (2000): Evaluation of the Acute scarring response to the implant of different types of biomaterial in the abdominal wall. J Mat Sc: Materials in the Medicine; 11(1): 25-9.
- [7] Choukroun, J., Diss, A. and Simonpieri, A. (2006): Platelet-rich fibrin (PRF): a second-generation platelet concentrate. Part V: histologic evaluations of PRF effects on bone allograft maturation in sinus lift. Oral Surg. Oral Med. Oral Pathol. Oral Radiol. Endodont. 101: 299–303.
- [8] Dohan, D. M., Choukroun, J., Diss, A., Dohan, S. L., Dohan, A. J. J., Mouhyi, J. and Bruno Gogly (2006) B: Platelet-rich fibrin (PRF): A second-generation platelet concentrate. Part III: Leucocyte activation: A new feature for platelet concentrates? Oral Surg Oral Med Oral Pathol Oral Radiol Endod. 10: 51-55.
- [9] Dohan, D. M., Choukroun, J., Diss, A., Dohan, S. L., Dohan, A. J. J., Mouhyi, J. and Bruno Gogly (2006) A: Platelet-rich fibrin (PRF): A second-generation platelet concentrate. Part I: Technological concepts and evolution. Oral Surg Oral Med Oral Pathol Oral Radiol Endod. 101: 37–44.
- [10] Dubcenco, E., Assumpcao, L., Dray, X., Gabrielson, K., Ruben, D., Pipitone, L., Donatelli., Krishnamurthy, D., Baker, J. and Marohn, M. (2009). Adhesion formation after peritoneoscopy with liver biopsy in a survival porcine model: comparison of laparotomy, laparoscopy, and transgastric natural orifice transluminal endoscopic surgery (NOTES). Endoscopy Journal; 41(11): 971 978.
- [11] Eryilamz, R.; Sahin, M. and Tekeliogu, M. H. (2006): Which repair in umbilical hernia of adult primary or mesh. Int Surg. 91: 258-261.
- [12] Escande Remi; Nizar Khelil; Isabelle Di Centa; Caroline Roques; Maguette Ba; Fatima Medjahed-Hamidi; Frederic Chaubet; Didier Letourneur; Emmanuel

- Lansac and Anne Meddahi-Pelle (2011): Pericardial Processing: Challenges, Outcomes and Future Prospects, Biomaterials Science and Engineering: 437-456.
- [13] Hafeez, Y. M., Zuki, A. Z., Logman, M. Y., Noordin, M. M. and Yusof, N. (2005): Comparative evaluation of the processed bovine tunica vaginalis implant in a rat model. Anat. Sci. Int. 80: 181-188.
- [14] Hafeez, Y. M., Zuki, A. Z., Logman, M. Y., Yusof, N., Asnah, H. and Noordin, M. M. (2004): Glycerol preserved bovine pericardium for abdominal wall reconstruction: experimental study in rat model. Med. J. Malaysia. 59: 117-118.
- [15] James, N. L., Poole-Warren, L. A, Schindhelm, K., Milthorpe, B. K., Mitchell, R. M., Mitchell, R. E., and Howlett, C. R. (1991): Comparative evaluation of treated bovine pericardium as a xenograft for hernia repair. Biomaterials 12: 801-807.
- [16] Kader, N. H., Abass, B. T. and Al-Sadi, H. I. (2005): A comparative experimental study of the use of tunica vaginalis and pericardium as allografts for hernioplasty in sheep. Iraqi J. Vet. Sci., 19: 57-70.
- [17] Kassem, M. M., El-Kammar, M. H., Korittum, A. S. and Abdel-Wahed, A. A. (2014): Using of Polypropylene Mesh for Hernioplasty in Calves Alexandria Journal of Veterinary Sciences, 40: 112-117.
- [18] Kumar, A., Mohindroo, J., Sangwan, V., Mahajan, S. K., Singh, K., Anand, A. And Saini, N. S. (2014): Ultrasonographic evaluation of massive abdominal wall swellings in cattle and buffaloes. Turkish Journal of Veterinary and Animal Sciences. 38: 100-103.
- [19] Kumar, N., Mathew, D. D., Gangwar, A. K., Remya, V., Muthalavi, M. A., Maiti, S. K., Sharma, A. K. (2014): Reconstruction of large ventrolateral hernia in a buffalo with acellular dermal matrix: a method for treating large hernias in animals. Vet. arhiv 84: 691-699.
- [20] Manzoor Dar, Tajamul Hakim, Ajaz Shah, Latief Najar, Gowhar Yaqoob, Faiqah Lanker. (2016): Use of autologous platelet-rich fibrin in osseous regeneration after cystic enucleation: A clinical study; Journal of Oral Biology and Craniofacial Research. 227-230.
- [21] Marmotti, A., Rossi, R., Castoldi, F., Roveda, E., Michielon, G. and Peretti, G. M. (2015): PRP and articular cartilage: a clinical update. Bio Med. Res. Int. 4 (2): 215-221.
- [22] Matthews, B. D., Pratt, B. L., Pollinger, H. S., Backus, C. L., Kercher, K. W., Sing, R. F. and Heniford, B. T. (2003): Assessment of adhesion formation to intraabdominal polypropylene mesh and polytetrafluoroethylene mesh. J. Surg. Res. 114 (2): 126-132.
- [23] Mustafa Tunali, Hakan Özdemir, Zafer Küçükodacı, Serhan Akman, Elif Öncü, Mustafa Aydınbelge, Melek Akman and Erhan Firatli (2016): A New Centrifugation Method for the Improvement of Platelet- Rich Fibrin

- Products: A preliminary Study. British Journal of Medicine and Medical Research. 13 (6): 1-10.
- [24] Schmidt, C. E. and Baier, J. M. (2000): Acellular vascular tissues: natural biomaterials for tissue repair and tissue engineering. Biomaterials, 21 (22): 2215–2231.
- [25] Schoen, F. J. and Levy, R. J. (1999): Tissue heart valves: current challenges and future research perspectives. J Biomed Mater Res, 47 (4): 439–465.
- [26] Shoukry, M., El-Keley, M., Hamouda, M. and Gadallah, S. (1997): Commercial polyester fabric repair of abdominal hernias and defects. Vet. Rec. 140: 606-607.
- [27] Sommers, K. E. and David, T. E. (1997): Aortic valve replacement with patch enlargement of the aortic annulus. Ann Thorac Surg, Vol. 63 (6): 1608-1612.
- [28] Takamura, M., Yasuda, T., Nakano, A. Shima, H. and Neo, M. (2017): The effect of platelet-rich plasma on Achilles tendon he 448 a ling in a rabbit model. Acta. Orthop. Traumatol. Turc.: 65–72.
- [29] Tsukiyama, K., Jezie, A., Acorda, Magr and Haruo yamada. (1996): Evaluation of Superficial Digital Flexor Tendinitis in Racing Horses Through Gray Scale Histogram Analysis of Tendon Ultrasonograms. Veterinary Radiology & Ultrasound, 37 (1): 46-50.
- [30] Van der Velden, M.A. and Klein, W.R. (1994): A modified technique for implantation of polypropylene mesh for the repair of external abdominal hernias in horses: a review of 21 cases. Vet. Quart. 16, Suppl. 2, S108-S110.
- [31] Van Eps, J., Fernandez-Moure, J., Cabrera, F., Wang, X., Karim, A., Corradetti, B., Tasciotti, E. and Weiner, B. (2016): Decreased hernia recurrence using autologous platelet-rich plasma (PRP) with Strattice™ mesh in a rodent ventral hernia model. Surg. Endosc.: 3239 3249.
- [32] Vilar, J. M., CORBERA, J. A. and Giuseppe Spinella. (2011): Double-layer mesh hernioplasty for repairing umbilical hernias in 10 goats. Turk. J. Vet. Anim. Sci. 35 (2): 131-135.

Tables:

- Table (1): Modified Hopkins adhesion score, adapted by **Dubcenco**, et. al., (2009).
- **Table (2):** Changes in Implant Gray Scale (IGS) Values in the Different Groups after Implantation.
- **Table (3):** Changes in Subcutaneous Gray Scale (SGS) Values in the Different Groups after implantation.
- **Table (4):** Changes in Skin Implant Distance (SID) Values in the Different Groups after Implantation.
- **Table (5):** Changes in Tensile Strength in the Different Groups at 8th and 12th weeks after implantation.

Table (6): Changes in Load at Failure Values in the Different Groups at 8th and 12th weeks after implantation.

Table (7): Changes in Strain (%) Values in the Different Groups at 2nd and 3rd months after implantation.

Table (8): Adhesion score in Different Tested Groups according to Modified Hopkins Adhesion Score.

Tables footnotes

Table (2): Data was presented as mean \pm Standard Error (SE). Values with different superscript numbers within the same column were significantly different at p < 0.001. Data with different superscript letters within the same row were significantly different at p < 0.001 and p < 0.0001.

Table (3): Data was presented as mean \pm Standard Error (SE). Values with different superscript numbers within the same column were significantly different at p < 0.001. Data with different superscript letters within the same row were significantly different at p < 0.001 and p < 0.0001.

Table (4): Data was presented as mean \pm Standard Error (SE). Values with different superscript numbers within the same column were significantly different at p < 0.001. Data with different superscript letters within the same row were significantly different at p < 0.001 and p < 0.0001.

Table (5): Data was presented as mean \pm Standard Error (SE). Values with different superscript letters within the same column were significantly different p < 0.001 at 8^{th} week and p < 0.0001 at 12^{th} week.

Table (6): Data was presented as mean \pm Standard Error (SE). Values with different superscript letters within the same column were significantly different p < 0.001 at 8th week and p < 0.0001 at 12th week.

Table (7): Data was presented as mean \pm Standard Error (SE). Values with different superscript letters within the same column were significantly different at p = 0.065 at 12^{th} week.

Legends of Figures:

Figure (1): Qualitative and quantitative ultrasonographic assessment of the prosthetic implants in different groups at 1st day, 1st, 2nd, 3rd, 4th, 8th and 12th weeks post implantation. Qualitative ultrasonogram (a), implant gray scale (b) and subcutaneous gray scale.

Figure (2): Tensiometric characters of the prosthetic implants in different groups at 8th and 12th weeks post implantation. Site of breakage or failure (white arrow).

Figure (3): Macroscopic picture of the parietal surface of the prosthetic implants in different groups at 4th, 8th and 12th weeks post implantation. Newly formed blood vessels (White arrows).

Figure (4): Macroscopic picture of the visceral surface of the prosthetic implants in different groups at 4th, 8th and 12th weeks post implantation. Newly formed blood vessels (White arrows).

Figure (5): Adhesion Score in different groups according to Modified Hopkins Adhesion Score. Score 0 with no adhesion (A), Score 1 with single filmy adhesion between the implant and the viscera (B), Score 2 with multiple filmy adhesions between the implant and the viscera (C), Score 3 with dense adhesions between the implant and the viscera (D), Score 4 with matted adhesions between the implant and the viscera (E).

Figure (6): Microscopic picture of native unprocessed bovine pericardium (A), Glycerolized Bovine Pericardium (GBP) (B) and Platelet Rich Fibrin (PRF). Single epithelial layer (Epi, red arrows), different levels of collagen organization (C, blue arrows), the fibroblasts (black arrows), few necrotic nuclei (yellow arrows), fibrin network (n), aggregates of blood platelets (white arrows). (H&E x40)

Figure (7): Microscopic picture of the prosthetic implants in different groups at 4th, 8th and 12th weeks post implantation. Intact structure of pericardial implant (yellow arrows), inflammatory cells infiltrations (green arrows), newly formed connective tissue (black arrows), neovascularization (blue arrows), elongated spindle shape fibroblasts surrounding collagen fibers (red arrows). (H&E x16)

Scor e	Frequency	Size/width (cm)	Density	Dissection
0	0	No adhesion	No adhesion	No adhesion
1	1	< 1	Single thin, filmy	Minimal blunt
			adhesion	dissection, tears easily
2	1-2	1-2	Multiple thin, filmy adhesions	Blunt dissection only
3	3-4	2-3	Dense adhesion(s) with or without filmy adhesions	Sharp dissection or electrocautery, no organ/serosal damage
4	4+	3+	Matted adhesion(s) with or without filmy adhesions	Sharp dissection or electrocautery, with unavoidable organ/serosal damage

Time	GBP Group	PPM Group	GBP-PRF Group	PPM-PRF Group
Day 1	145.34 ± 2.13 b 1	166.59 ± 2.64 a 1	137.39 ± 2.23 c 2	107.44 ± 1.72 d ²
Week 1	70.15 ± 3.39 b 4	46.04 ± 3.06 c 6	90.50 ± 4.85 a 4	$100.73 \pm 0.58a^3$
Week 2	88.24 ± 5.88 b 3	75.17 ± 2.34 c 5	94.91 ± 1.67 a b 3	103.40 ± 4.28 a ²
Week 3	93.26 ± 2.77 b 2 3	89.03 ± 1.62 b 4	114.49 ± 2.65 a 3	111.72 ± 0.80 a 2
Week 4	108.63 ± 11.93 a	97.31 ± 3.50 a 3	136.52 ± 10.83 a	114.40 ± 4.37 a b
Week 8	128.33 ± 6.31 b 1	105.57 ± 1.47 c ²	166.23 ± 1.68 a 1	129.00 ± 1.08 b 1
Week 12	135.49 ± 1.93 b 1	112.22 ± 2.42 b 2	177.88 ± 12.88 a	129.56 ± 6.98 b 1

Time	GBP Group	PPM Group	GBP-PRF Group	PPM-PRF Group
Day 1	68.95 ± 3.68 b 1	110.33 ± 6.77 a 1	54.32 ± 2.33 b 4	97.64 ± 6.77 a 1
Week 1	16.42 ± 0.56 b 3	38.77 ± 0.65 a 5	35.25 ± 3.13 a 5	53.43 ± 10.21 a 3
Week 2	17.21 ± 0.99 c 3	41.91 ± 1.57 b 5	41.93 ± 2.68 b 5	75.44 ± 9.39 a 2
Week 3	19.40 ± 1.07 c ³	49.12 ± 3.04 b 5	60.27 ± 5.46 b 3 4	85.82 ± 1.10 a 1 2
Week 4	22.46 ± 2.05 d 3	60.26 ± 2.18 b 4	67.69 ± 4.33 b 2 3	94.19 ± 5.94 a 1 2
Week 8	40.90 ± 1.75 d ²	82.54 ± 2.19 b 3	71.11 ± 1.13 c ²	97.41 ± 2.46 a 1
Week 12	64.18 ± 6.15 b 1	98.62 ± 3.43 a 2	99.53 ± 2.06 a 1	104.42 ± 3.44 a 1

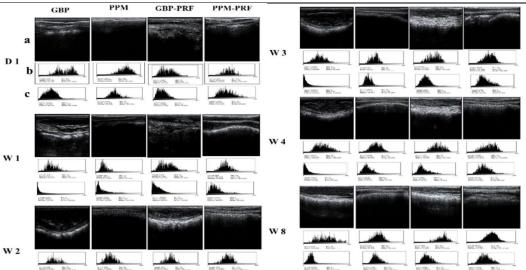
Time	GBP Group	PPM Group	GBP-PRF Group	PPM-PRF Group
Day 1	4.00 ± 0.40 a 4	1.17 ± 0.09 c 4	5.00 ± 0.58 a 3 4	2.58 ± 0.36 b 2 3 4
Week 1	18.00 ± 1.15 a 1	4.73 ± 0.29 c 1	9.08 ± 0.30 b 1	4.00 ± 0.29 c 1
Week 2	16.83 ± 0.93 a 1	4.13 ± 0.18 c ²	8.50 ± 0.29 b 1	3.00 ± 0.14 c ²
Week 3	15.50 ± 0.76 a 1	3.83 ± 0.12 c ²	6.50 ± 0.29 b 2	2.75 ± 0.14 c 2 3
Week 4	15.33 ± 0.88 a 1	3.23 ± 0.12 c ³	5.90 ± 0.06 b 2 3	2.68 ± 0.09 c 2 3
Week 8	11.00 ± 0.58 a ²	3.03 ± 0.09 c 3	5.13 ± 0.09 b 3 4	2.20 ± 0.12 c 3 4
Week 12	7.33 ± 1.45 a 3	2.77 ± 0.15 b 3	4.50 ± 0.29 b 4	1.97 ± 0.20 b 4

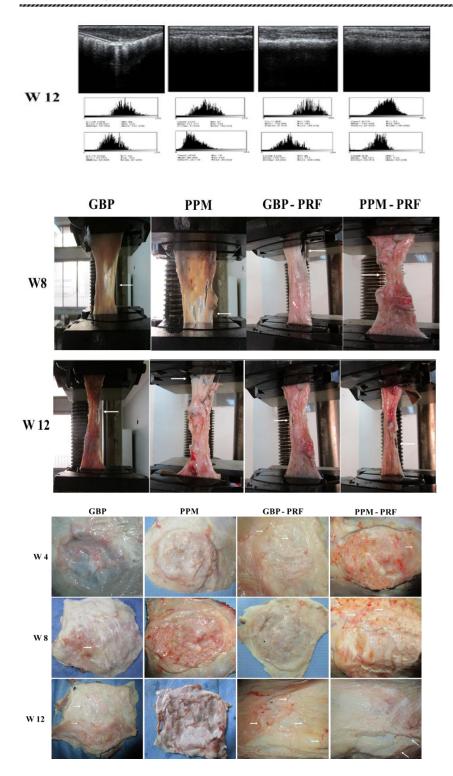
Time	Week 8	Week 12	
GBP Group	19.27 ± 0.43 b	26.13 ± 0.47 b	
PPM Group	20.67 ± 1.20 ^b	26.33 ± 0.88 b	
GBP-PRF Group	27.20 ± 1.42^{a}	33.10 ± 0.83 a	
PPM-PRF Group	28.33 ± 0.88^{a}	34.03 ± 1.28 a	

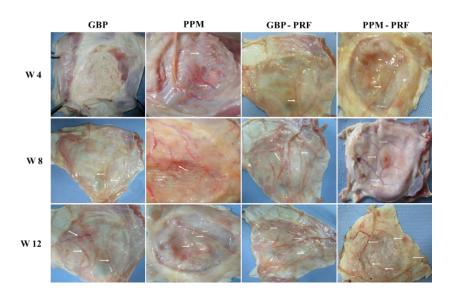
Time	Week 8	Week 12
GBP Group	83.80 ± 0.92 b	96.87 ± 0.86 b
PPM Group	85.77 ± 1.69 ^b	97.57 ± 0.87 b
GBP-PRF Group	93.67 ± 1.45 a	102.43 ± 2.31 a
PPM-PRF Group	96.10 ± 2.28 a	104.67 ± 0.88 a

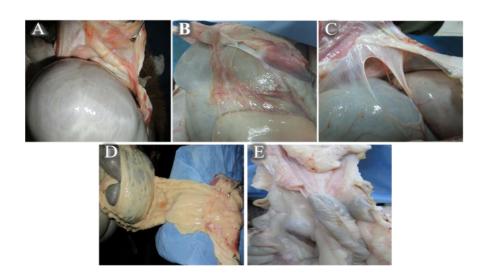
Time	Week 8	Week 12
GBP Group	41.83 ± 1.98	47.67 ± 1.45 a
PPM Group	40.90 ± 1.05	45.43 ± 1.79
GBP-PRF Group	44.83 ± 1.09	48.43 ± 0.45 a
PPM-PRF Group	41.67 ± 0.68	43.37 ± 0.52 b

Adhesion	GBP Group		PPM Group		GBP-PRF Group			PPM-PRF Group				
Score	W	W	W	W	W	W	W	W	W	W	W	W
	4	8	12	4	8	12	4	8	12	4	8	12
0									2			1
1	1	2	3			1	3	2	1	1	2	2
2	1	1			2	1		1		2	1	
3	1			2	1	1						
4				1								









W 12

